Commun Nonlinear Sci Numer Simulat 150 (2025) 109010

Contents lists available at ScienceDirect

Communications in Nonlinear Science and Numerical Simulation

journal homepage: www.elsevier.com/locate/cnsns

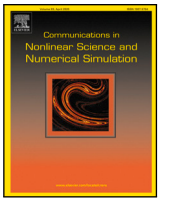

Research paper

Event-based uniform prescribed-time output feedback control for irregular output-constrained nonlinear systems

Yangang Yao [a], Yu Kang [b,*], Yunbo Zhao [b], Jieqing Tan [c], Lichuan Gu [a,*], Chao Wang [a]

[a] School of Information and Artificial Intelligence, Anhui Agricultural University, Hefei, 230036 China
[b] Department of Automation, University of Science and Technology of China, Hefei, 230027, , China
[c] School of Mathematics, Hefei University of Technology, Hefei 230601, China

ARTICLE INFO

Keywords:
Irregular output constraints
Prescribed-time output feedback control
Event trigger
Fuzzy logic system

ABSTRACT

This paper proposes an event-based uniform prescribed-time output feedback control (PTOFC) approach for irregular output-constrained nonlinear systems (OCNSs). Unlike the most existing methods of OCNSs, they mainly focus on OCNSs with infinite-time/deferred output constraints (i.e., the output constraints existing for all $t \geq 0$ or $t \geq t_0$), while many actual systems often suffer from irregular output constraints (including infinite-time constraints, deferred constraints, unconstrained, constrained and unconstrained alternations, etc.), leading to new challenges in control design. By devising a stretch model-based nonlinear mapping function, and combining with event trigger control (ETC) technique, an event-based unified output feedback control algorithm is proposed, and the significant advantage is its suitability for infinite-time/deferred/alternant OCNSs, as well as unconstrained systems, without necessitating modifications to the control structure, and the communication burden is also effectively reduced. Furthermore, with the aid of the scaling transformation function (STF)-based prescribed-time stability (PTS) criteria, a novel prescribed-time state observer (PTSO)-based PTOFC algorithm is designed, under which the settling time can be pre-set arbitrarily regardless of the initial system states and control parameters. Meanwhile, the problems of singularity and large initial control input in conventional prescribed-time control schemes are eliminated. The presented approach is verified by means of simulation examples.

1. Introduction

Due to users' special needs for control performance, physical limitations or production safety, the control for OCNSs has become a rapidly emerging topic in the last few decades. The barrier Lyapunov function (BLF)-based approach [1] has garnered great attention since its inherent merits of low computational complexity and absence of optimization requirements. For instance, with the help of symmetric/asymmetric log/tan-type BLFs, the control algorithms for symmetric (or asymmetric) OCNSs with different forms were proposed in [2–8]. Another popular method for dealing with constraint problems is called the nonlinear mapping function (NMF)-based methods, see [9–15] and references. The NMF-based methods innovatively establish a nonlinear mapping between output/state variables and auxiliary variables on the constraint interval to the set of real numbers, and then control the auxiliary variables to ensure that the constraints are obeyed. The merit of the NMF-based approach over the BLF-based approach is that

* Corresponding authors.
E-mail addresses: ygyao@ustc.edu.cn (Y. Yao), kangduyu@ustc.edu.cn (Y. Kang), ybzhao@ustc.edu.cn (Y. Zhao), jieqingtan@hfut.edu.cn (J. Tan), glc@ahau.edu.cn (L. Gu), wangchaoicle@ahau.edu.cn (C. Wang).

https://doi.org/10.1016/j.cnsns.2025.109010
Received 19 November 2024; Received in revised form 21 March 2025; Accepted 27 May 2025
Available online 4 June 2025

the intermediate control function does not need to meet any constraints. It is noteworthy that the majority of current approaches mainly focus on nonlinear systems with infinite-time constraints (i.e., the constraints always exist), which do not fit with many practical scenarios. Towards this end, the recent advancements in control methods for deferred OCNSs [16–18] have overcome the above limitations to a certain extent, and even enable achieving global stability. In practice, however, the system may also often suffer from irregular output constraints (including infinite-time constraints, deferred constraints, unconstrained, constrained and unconstrained alternations, etc.). As an illustrative example, in addition to the usual infinite time/deferred constraints, the UAV encounters constraints only within specific areas when navigating through multiple narrow passages for a rescue mission, rather than throughout the entire operation. Evidently, the control design for irregular OCNSs is more challenging, and has wider practical application requirements. Recently, some novel approaches of irregular output/state-constrained nonlinear systems [19–22] were presented. Nevertheless, the above methods are based on the premise that all states can be measured, which inspires us to further study the output feedback control algorithm for irregular OCSNs.

Due to limitations in cost, accuracy and measurement instruments, the state variables of actual systems are often unmeasurable. It is evident that the state-feedback control algorithms of OCNSs are not suitable for the OCNSs with unmeasurable states. As a result, the state observer-based output feedback control algorithms were presented for OCNSs, see [23–30] and related references. For instance, by means of state observer and tan-type BLFs, two output feedback control methods were presented for output-constrained robotic systems [23,24]. With the aid of log-type BLFs, the output feedback control methods for OCNSs with finite/fixed/predefined-time convergence were presented in [25–27],respectively. Recently, some novel output feedback control schemes of OCNSs with deferred output constraints were proposed in [28–30], which can achieve the global performance. It should be noted that all the above methods are still limited to OCNSs with infinite-time/deferred output constraints, so investigating the output feedback control of irregular OCNSs poses a formidable yet meaningful pursuit.

As is widely acknowledged, the attainment of system stability within a limited time holds significant value. Towards this end, the finite-time control (FTC) [24,25,31,32] and the fixed-time control (FxTC) [10–13,17,26,33–35] were obtained for nonlinear constrained systems. The existing FTC and FxTC methods, however, have limitations in which the settling time is contingent upon initial system states and control parameters, thereby greatly diminishing their practical application in control systems. Afterwards, the prescribed-time control (PTC) first presented in [36] has garnered significant attention, its most notable advantage is the ability to arbitrarily pre-set settling time regardless of the initial system states and control parameters. As a result, numerous effective PTC algorithms emerged. For example, the STF-based PTC algorithms of uncertain nonlinear systems [37,38], switched systems [39], multi-agent systems [40], high-order systems [41], and stochastic systems [42,43] were obtained. What calls for special attention is that the STF in [37–43] is infinite at the prescribed time, which may result in the singularity during implementation of the constructed controllers. Therewith, a novel practical PTC algorithm was presented [44], which avoids the singularity problem. Inspired by [44], Zeng et al. [45] presented a PTOFC algorithm for switched systems. Nevertheless, the prescribed-time stability (PTS) of [44,45] should follow the following harsh condition: $\dot{\mathscr{L}} \leq -\mathscr{C}(t)\mathscr{L}$ (where $\mathscr{C}(t)$ and $\mathscr{L}$ represent time-varying function and Lyapunov function (LF), respectively). Recently, some novel more relaxed criterion-based PTC algorithms were obtained in [46–49]. For instance, Wang et al. [46,47] proposed two event-based practical PTC algorithms, where the following condition should be satisfied: $\dot{\mathscr{L}} \leq -k\mathscr{L} - \left(2\dot{\mathscr{C}}(t)/\mathscr{C}(t)\right)\mathscr{L} + \eta/\mathscr{C}(t) + \delta$, $\mathscr{C}(t)$ stands for a piecewise time-varying function, $k, \eta, \delta \in R^{+}$. The presence of $\eta/\mathscr{C}(t)$, however, still leads to singularity. In addition, the practical PTC algorithms without singularity were recently proposed in [48,49], where the following condition should be satisfied: $\dot{\mathscr{L}} \leq -(\pi/rT)(\mathscr{L}^{1+r/2} + \mathscr{L}^{1-r/2}) + \delta$ with $r, T, \delta \in R^{+}$. Note that the inclusion of a term with an exponent greater than 1 in the designed control input leads to a large initial control input. Recently, two newly STF-based PTOFC approaches were proposed in [50,51], which can effectively overcome large initial control input and singularity problem. Note that the STF designed in [50,51] is relatively complex, and the methods proposed in [50,51] are triggered based on time, causing a waste of communication resources to a certain extent, which drives us to investigate a novel event-based PTOFC approach of irregular OCNSs.

According to the preceding discussion, this article centers on the event-based uniform PTOFC issue of irregular OCNSs, which has yet to be resolved in previous research. Conclude the contributions as follows

(1) Different from most existing methods for OCNSs [23–30], they mainly focus on OCNSs with infinite-time/deferred output constraints, the irregular output constraints that this article focuses on include infinite-time constraints, deferred constraints, unconstrained, constrained and unconstrained alternations, and so on, which is much more complex than the infinite-time/deferred output constraints, and closer to the many actual systems. By devising a stretch model-based NMF, the irregular output constraints are processed uniformly, and the significant advantage of the presented approach is its suitability for OCNSs with infinite-time/deferred/alternate output constraints, and unconstrained systems, without necessitating modifications to the control structure.

(2) With the aid of the STF-based PTS criteria, a novel PTSO-based PTOFC algorithm for irregular OCNSs is designed. The proposed algorithm guarantees that the settling time of the observation system and the control system can be pre-set arbitrarily regardless of the initial states or control parameters. Meanwhile, the problems of singularity [37–43,46,47] and large initial control inputs [48,49] in conventional PTC algorithms are eliminated. Furthermore, the introduction of the relative threshold-based ETC technique also saves network resources effectively.

2. Problem statement and preliminaries

2.1. Problem statement

Consider the following irregular OCNSs

$$\begin{cases} \dot{x}_i = x_{i+1} + f_i\left(\bar{x}_i\right), i = 1, \ldots, n-1 \\ \dot{x}_n = u + f_n\left(\bar{x}_n\right) \\ y = x_1 \end{cases} \tag{1}$$

where $\bar{x}_n = \left[x_1, \ldots, x_n\right]^{\mathrm{T}}$ stands for system state vector, $\bar{x}_i = \left[x_1, \ldots, x_i\right]^{\mathrm{T}}$, y, u stand for system output and input, respectively, and $x_i (i \geq 2)$ is unmeasured. $f_i(\cdot)$ represents uncertain nonlinear continuous function with $i = 1, \ldots, n$. The irregular output constraints need to be obeyed, i.e., $x_1 \in \mathscr{B}_{x_1}$, where

$$\mathscr{B}_{x_1} = \left\{ x_1 \in R \middle| \underline{\mathscr{B}}(t) < x_1 < \bar{\mathscr{B}}(t), \forall t \in [t_{s,j}, t_{e,j}] \right\} \tag{2}$$

where $\bar{\mathscr{B}}(t)$ and $\underline{\mathscr{B}}(t)$ represent the upper and lower constraint boundaries respectively, satisfying $\underline{\mathscr{B}}(t) < 0 < \bar{\mathscr{B}}(t)$, $0 \leq t_{s,j} \leq t_{e,j} \leq \infty$ with $j = 1, \ldots, m$.

Remark 1. The irregular output constraints considered in this article include the following constraint types:

T-1: infinite-time output constraints, i.e., $t_{s,1} = 0, t_{e,1} = \infty$;

T-2: deferred output constraints, i.e., $t_{s,1} = t_0 > 0, t_{e,1} = \infty$;

T-3: without output constraints, i.e., $t_{s,1} = \infty$;

T-4: alternate between constrained and unconstrained, such as "constrained→unconstrained→ constrained" ($0 = t_{s,1} < t_{e,1} < t_{s,2} < t_{e,2} = +\infty$); "unconstrained→ constrained→ unconstrained" ($0 < t_{s,1} < t_{e,1} < t_{s,2} = +\infty$), and so on.

Evidently, the control design of irregular OCNSs poses greater challenges. In particular, it is more challenging to construct a unified control framework to guarantee that it is suitable for a variety of irregular OCNSs (including (T-1)-(T-4)) without changing the control structure. This article takes a step forward towards addressing this issue.

The objective of this article is to develop an event-based unified PTOFC algorithm that ensures semi-global boundedness of system (1) with $x_1(0) \in \mathscr{B}_{x_1}$, while also satisfying the irregular output constraints. Meanwhile, the system output is capable of tracking the reference signal y_d within a specified time.

The following assumptions are posited.

Assumption 1. y_d is bounded and differentiable, and $y_d \in \left(\underline{\mathscr{B}}(t), \bar{\mathscr{B}}(t)\right)$ for $\forall t \in [t_{s,j}, t_{e,j}]$.

Assumption 2. For $\forall \chi_1, \chi_2 \in R^i$, and $f_i(\cdot)$ in system (1), there exist a set of constants b_i such that $\left|f_i(\chi_1) - f_i(\chi_2)\right| \leq b_i \left\|\chi_1 - \chi_2\right\|$.

2.2. STF-based prescribed-time stability (PTS) criteria

Lemma 1 ([20]). *Give the following system*

$$\dot{x} = f(x, t), \quad f : R^m \times R^+ \to R^m \tag{3}$$

with $f(\mathbf{0}, t) = 0$, $x = \mathbf{0}$ be the solution of system (3). If $\exists k, \delta \in R^+$, such that the LF $\mathscr{L}(t)$ satisfies

$$\dot{\mathscr{L}}(t) \leq -k\mathscr{L}(t) - \frac{\dot{\mathscr{C}}(t)}{\mathscr{C}(t)}\mathscr{L}(t) + \delta \tag{4}$$

then, when $t \geq t_f$, $\mathscr{L}(t) \leq \varepsilon\mathscr{L}(0) + \delta/k$, and $\mathscr{L}(t) \to \delta/k$ as $t \to +\infty$, i.e., the solution of (3) is practical prescribed time stable, where $\mathscr{C}(t)$ denoted the STF, as defined below

$$\mathscr{C}(t) = \begin{cases} \frac{1}{(1-\varepsilon)(1-t/t_f)^n + \varepsilon}, & t \in [0, t_f) \\ 1/\varepsilon, & t \in [t_f, +\infty) \end{cases} \tag{5}$$

where n is the order of the system, t_f and $0 < \varepsilon \ll 1$ denote positive design parameters.

It is evident that $\mathscr{C}(t)$ possesses the following characteristics:

(i) $\mathscr{C}(t)$ is non-decreasing and continuous on $[0, +\infty)$, and $\mathscr{C}(0) = 1$, $\mathscr{C}\left(t_f\right) = 1/\varepsilon$;

(ii) $\mathscr{C}(t)$ is C^n on $[0, +\infty)$.

Remark 2. It should be noted that the STF designed in [37–43] (like $\mathscr{C}(t) = t_f/(t_f - t)$ and its deformation) approaches to infinity as $t \to t_f$, which may result in a singularity problem during implementation of the constructed controllers. The PTS criterion presented in [46,47], requires satisfaction of $\dot{\mathscr{L}} \leq -(k + 2\dot{\mathscr{C}}(t)/\mathscr{C}(t))\mathscr{L} + \eta/\mathscr{C}(t) + \delta$ with $k, \eta, \delta \in R^+$. The presence of $\eta/\mathscr{C}(t)$, however, still leads to singularity. The PTS criterion presented in [48,49] requires satisfaction of $\dot{\mathscr{L}} \leq \left(\pi/(rt_f)\right)\left(\mathscr{L}^{1+r/2} + \mathscr{L}^{1-r/2}\right) + \delta$ with

$t_f, \delta \in R^+, r \in (0,1)$. For the methods proposed in [48,49], the inclusion of a term with an exponent greater than 1 in the designed control input leads to a large initial control input. In other words, under the same initial conditions, the presented PTOFC algorithm can achieve the same control performance of that in [48,49] under the premise of smaller control input.

2.3. Fuzzy logic system (FLS)

Lemma 2 ([10]). *The FLS can be utilized for the purpose of approximating a nonlinear uncertain function $\mathcal{F}(\mathcal{Z})$, i.e.,*

$$\mathcal{F}(\mathcal{Z}) = Y^{\mathrm{T}}\Omega(\mathcal{Z}) + \phi(\mathcal{Z}), \quad (|\phi(\mathcal{Z})| \le \phi, \phi \in R^+) \tag{6}$$

where Y, $\Omega(\mathcal{Z}) = [\Omega_1(\mathcal{Z}), \ldots, \Omega_m(\mathcal{Z})]^{\mathrm{T}} / \sum_{j=1}^{m} \Omega_j(\mathcal{Z})$, $\phi(\mathcal{Z})$, $\mathcal{Z}$ stand for weight, basis function, error and input, respectively, $m \in R^+$. $\Omega_i(\mathcal{Z})$ is selected as

$$\Omega_i(\mathcal{Z}) = \exp\left[\frac{-\left(\mathcal{Z}-\vartheta_i\right)^{\mathrm{T}}\left(\mathcal{Z}-\vartheta_i\right)}{\iota_i^{\,2}}\right], i = 1, \ldots, m \tag{7}$$

where ϑ_i and ι_i denote the spreads and the center vector of $\Omega_i(\mathcal{Z})$.

3. Main results

3.1. Prescribed-time state observer (PTSO)

Design the PTSO as follows

$$\begin{cases} \dot{\hat{x}}_i = \hat{x}_{i+1} + l_i \mathscr{C}_0^i \left(x_1 - \hat{x}_1\right), i = 1, \ldots, n-1 \\ \dot{\hat{x}}_n = u + l_n \mathscr{C}_0^n \left(x_1 - \hat{x}_1\right) \end{cases} \tag{8}$$

where $\mathscr{C}_0 = \bar{k}\left(\bar{k}_0 + \dot{\mathscr{C}}(t)/\mathscr{C}(t)\right)$, $\bar{k}$ and $\bar{k}_0$ are positive design parameters, satisfying $\bar{k}\bar{k}_0 \le 1$, and $l_i > 0$ $(i = 1, \ldots, n)$ are suitably selected to ensure the polynomial $a^n + l_1 a^{n-1} + \cdots + l_{n-1}a + l_n$ is Hurwitz. Therefore, for $\forall \epsilon \in R^+$, $\exists B = B^{\mathrm{T}}$ satisfying

$$A^{\mathrm{T}}B + BA \le -(n+1)I, \quad DB + BD \ge 0 \tag{9}$$

where

$$D = \begin{bmatrix} \epsilon & 0 & \cdots & 0 \\ 0 & 1+\epsilon & \cdots & 0 \\ \vdots & \vdots & \ddots & \vdots \\ 0 & 0 & \cdots & n-1+\epsilon \end{bmatrix}, A = \begin{bmatrix} -l_1 & 1 & \cdots & 0 \\ \vdots & \vdots & \ddots & \vdots \\ -l_{n-1} & 0 & \cdots & 1 \\ -l_n & 0 & \cdots & 0 \end{bmatrix}.$$

Let $\tilde{x}_i = x_i - \hat{x}_i$, and the following coordinate transformation is introduced

$$\eta_i = \frac{\tilde{x}_i}{\mathscr{C}_0^{i-1+\epsilon}}, i = 1, \ldots, n. \tag{10}$$

From (1) and (8)–(10), one has

$$\dot{\eta} = \mathscr{C}_0 A\eta + F + \Delta F - \frac{\dot{\mathscr{C}}_0}{\mathscr{C}_0} D\eta \tag{11}$$

where $F = \left[F_1, \ldots, F_n\right]^{\mathrm{T}}$ with $F_i = f_i(\bar{\hat{x}}_i)/\mathscr{C}_0^{i-1+\epsilon}$ and $\bar{\hat{x}}_i = \left[\hat{x}_1, \ldots, \hat{x}_n\right]^{\mathrm{T}}$, $\Delta F = \left[\Delta F_1, \ldots, \Delta F_n\right]^{\mathrm{T}}$ with $\Delta F_i = (f_i(\bar{x}_i) - f_i(\bar{\hat{x}}_i))/\mathscr{C}_0^{i-1+\epsilon}$, $\eta = \left[\eta_1, \ldots, \eta_n\right]^{\mathrm{T}}$.

Choose the LF as follows

$$\mathscr{L}_0 = \eta^{\mathrm{T}} B \eta. \tag{12}$$

According to (12), one has

$$\dot{\mathscr{L}}_0 \le -(n+1)\mathscr{C}_0 \|\eta\|^2 + 2\eta^{\mathrm{T}} BF + 2\eta^{\mathrm{T}} B\Delta F. \tag{13}$$

On the basis of the mean inequality, we have

$$2\eta^{\mathrm{T}} BF \le \|\eta\|^2 + \|B\|^2 \left[\frac{f_1^2(\hat{x}_1)}{\mathscr{C}_0^{2\epsilon}} + \cdots + \frac{f_n^2(\bar{\hat{x}}_n)}{\mathscr{C}_0^{2n-2+2\epsilon}}\right]. \tag{14}$$

Let $L\left(\bar{\hat{x}}_n\right) = \|B\|^2 \left[f_1^2(\hat{x}_1)/\mathscr{C}_0^{2\epsilon} + \cdots + f_n^2(\bar{\hat{x}}_n)/\mathscr{C}_0^{2n-2+2\epsilon}\right]$, and use the FLS to approximate it as follows

$$L\left(\bar{\hat{x}}_n\right) = Y^{\mathrm{T}}\Omega\left(\bar{\hat{x}}_n\right) + \phi\left(\bar{\hat{x}}_n\right) \tag{15}$$

where Y is the unknown weight vector, $\Omega\left(\bar{\hat{x}}_n\right)$ represents the bounded basis function satisfying $\|\Omega\left(\bar{\hat{x}}_n\right)\| \le 1$, and $\phi\left(\bar{\hat{x}}_n\right)$ denotes the FLS approximation error satisfying $\phi\left(\bar{\hat{x}}_n\right) \le \phi_0$, ϕ_0 is unknown constant.

Let $\Theta = \max_{1\le i\le n}\left\{2\|B\|\sum_{j=i}^{n} b_j/\mathscr{C}_0^{j-i}\right\}$, according to Assumption 2, one can obtain

$$\begin{aligned}2\eta^{\mathrm{T}}B\Delta F &\le 2\|\eta\|\|B\|\left(|\Delta F_1|+\cdots+|\Delta F_n|\right)\\ &\le 2\|\eta\|\|B\|\left(\frac{b_1}{\mathscr{C}_0^{\epsilon}}|\tilde{x}_1|+\cdots+\frac{b_n}{\mathscr{C}_0^{n-1+\epsilon}}\sum_{j=1}^{n}|\tilde{x}_j|\right)\\ &\le \Theta\|\eta\|\left(|\eta_1|+\cdots+|\eta_n|\right)\\ &\le \Theta\|\eta\|^2.\end{aligned} \tag{16}$$

Let $\bar{k} > \lambda_{\max B}/(n+1)$ and $k_0 = (n+1)\bar{k}_0 - (1+\Theta)/\lambda_{\min B} > 0$, where $\lambda_{\max B}$ and $\lambda_{\min B}$ represent, respectively, the maximum eigenvalue and minimum eigenvalue of B. Then, one has

$$\begin{aligned}\dot{\mathscr{L}}_0 &\le -(n+1)\mathscr{C}_0\|\eta\|^2+(1+\Theta)\|\eta\|^2+Y^{\mathrm{T}}\Omega\left(\tilde{x}_n\right)+\phi\left(\tilde{x}_n\right)\\ &\le -\frac{(n+1)\mathscr{C}_0}{\lambda_{\max B}}\eta^{\mathrm{T}}B\eta+\frac{1+\Theta}{\lambda_{\min B}}\eta^{\mathrm{T}}B\eta+\|Y\|+\phi\\ &\le -\left(k_0+\frac{\dot{\mathscr{C}}(t)}{\mathscr{C}(t)}\right)\mathscr{L}_0+\Delta_0\end{aligned} \tag{17}$$

where $\Delta_0 = \|Y\|+\phi$.

Remark 3. According to Lemma 1 and (17), one can know that $\mathscr{L}_0 \le \varepsilon\mathscr{L}_0(0)+\delta/k_0$ when $t\ge t_f$, and $\mathscr{L}_0(t)\to\delta/k_0$ as $t\to+\infty$. Based on the expression of $\mathscr{L}_0$, one can know that η_i converges to a neighborhood centered on zero when $t\ge t_f$. According to (10) and $\bar{k}_0\bar{k}\le 1$, one can further obtain $|\tilde{x}_i|\le|\eta_i|$ for $t\ge t_f$, which means that $\tilde{x}_i$ converges to a neighborhood centered on zero when $t\ge t_f$. It is worthy of noting that the majority of existing output feedback control methods for OCNSs do not take into account the setting time of state estimation error, with the exception of those presented in [26,42,43,50]. While the settling time of [26] is contingent upon several control parameters, the approaches designed in [42,43] exist the singularity problem, and the STF designed in [50] is relatively complex, and the PTSO designed in [50] is only suitable for second-order systems.

3.2. Prescribed-time output feedback control (PTOFC)

Firstly, a stretching function is designed as follows

$$\mathscr{S}(t) = \begin{cases} e^{\zeta_1(t)}, & t\in[0,t_{s,1})\\ 1, & t\in[t_{s,j},t_{e,j}),j=1,\ldots,m\\ e^{\zeta_{j+1}(t)}, & t\in[t_{e,j},t_{s,j+1}),j=1,\ldots,m-1\\ e^{\zeta_{k+1}(t)}, & t\in[t_{e,k},+\infty)\end{cases} \tag{18}$$

where

$$\begin{aligned}\zeta_1(t) &= -\frac{\left(t-t_{s,1}\right)^{2n}}{\sigma_1},\zeta_{m+1}(t) = -\frac{\left(t_{e,k}-t\right)^{2n}}{\sigma_{m+1}},\\ \zeta_{j+1}(t) &= \frac{1}{\sigma_{j+1}}\left[\frac{-2n\left(2t-t_{e,j}-t_{s,j+1}\right)^{2n+1}}{\left(t_{s,j+1}-t_{e,j}\right)^{2n+1}}\mathrm{sgn}(\cdot)+\frac{(2n+1)\left(2t-t_{e,j}-t_{s,j+1}\right)^{2n}}{\left(t_{s,j+1}-t_{e,j}\right)^{2n}}-1\right]\end{aligned}$$

with $j=1,\ldots,m-1$, $\mathrm{sgn}(\cdot)=\mathrm{sgn}(2t-t_{e,j}-t_{s,j+1})$, $0<\sigma_j\ll 1$ stands for the design constant. It is not difficult to see that the convergence rate of $\mathscr{S}(t)$ in the neighborhood near the segment point becomes faster with the decrease of σ_j.

According to (18), one know that $\mathscr{S}(t)$ exhibits the following characteristics:

(i) $\mathscr{S}(t)\equiv 1$ for $\forall t\in[t_{s,j},t_{e,j}]$, and $\mathscr{S}(t)\to 1$ when $t\to t_{s,j}{}^{-}$ or $t\to t_{e,j}{}^{+}$;

(ii) when t belongs to a large measure subset of $(0,t_{s,1})\cup\ldots(t_{e,j},t_{s,j+1})\cdots\cup(t_{e,k},+\infty), j=1,\ldots,m-1$, $\mathscr{S}(t)\to 0$;

(iii) $\dot{\mathscr{S}}(t)$ is continuous, and $\mathscr{S}(t)\in(0,1]$ for $\forall t\ge 0$.

Let $\chi_1 = x_1\mathscr{S}(t)$. Then, design the following stretch model-based NMF

$$\xi = \frac{x_1}{\left(\chi_1-\underline{\mathscr{B}}(t)\right)\left(\bar{\mathscr{B}}(t)-\chi_1\right)} \tag{19}$$

It is easy to obtain from (19) that if $\underline{\mathscr{B}}(0)<\chi_1(0)<\bar{\mathscr{B}}(0)$, then $\xi\to\infty$ only and only if $\chi_1\to\underline{\mathscr{B}}^{-}(t)$ or $\chi_1\to\bar{\mathscr{B}}^{+}(t)$. Then, one can further obtain that if ξ is bounded, and $\underline{\mathscr{B}}(0)<\chi_1(0)<\bar{\mathscr{B}}(0)$, then

$$\underline{\mathscr{B}}(t)<\chi_1<\bar{\mathscr{B}}(t). \tag{20}$$

Based on (20), we can further obtain

$$\frac{\underline{\mathscr{B}}(t)}{\mathscr{S}(t)}<x_1<\frac{\bar{\mathscr{B}}(t)}{\mathscr{S}(t)}. \tag{21}$$

Remark 4. According to the properties of $\mathscr{S}(t)$ and (21), one know that for $\forall t \in [t_{s,j}, t_{e,j}]$, $j = 1, \ldots, m$, $\underline{\mathscr{B}}(t) < x_1 < \bar{\mathscr{B}}(t)$ holds, i.e., the irregular output constraints are not violated; and when t belongs to a large measure subset of $(0, t_{s,1}) \cup \ldots (t_{e,j}, t_{s,j+1}) \cdots \cup (t_{e,k}, +\infty)$, the constraint boundaries $\underline{\mathscr{B}}(t)/\mathscr{S}(t)$ and $\bar{\mathscr{B}}(t)/\mathscr{S}(t)$ tend to infinity, i.e., $-\infty < x_1 < +\infty$. It should be emphasized that the function $\mathscr{S}(t)$ serves as a "stretching" mechanism for extending the original constraint boundaries to the infinite boundaries in situations where no constraints are necessary.

Remark 5. Note that the conventional output feedback control algorithms for OCNSs [23–30] are only applicable to OCNSs with infinite-time/deferred output constraints (i.e., the output constraints existing for all $t \geq 0$ or $t \geq t_0$). In this article, the stretch model-based NMF (19) is innovatively designed to establish the "continuous" switch between constrained and unconstrained, thus providing a complete framework for irregular OCNSs. In fact, by simply adjusting the parameters, the proposed method can be reduced to the results of [23–30,52,53] (see Remark 6). Although the latest methods proposed in [19–22] have made some breakthroughs, which also suit for irregular OCNSs. However, the above approaches are limited to OCNSs that all states can be measured, but not suit for irregular OCNSs with unmeasurable state.

For the sake of simplicity, in the subsequent sections, let $\underline{\mathscr{B}} = \underline{\mathscr{B}}(t), \bar{\mathscr{B}} = \bar{\mathscr{B}}(t), \mathscr{S} = \mathscr{S}(t)$.

Let $z_1 = \xi - \alpha_0, z_i = \hat{x}_i - \alpha_{i-1}, i = 2, \ldots, n$ with $\alpha_0 = y_d / \left(y_d \mathscr{S} - \underline{\mathscr{B}}\right)\left(\bar{\mathscr{B}} - y_d \mathscr{S}\right)$. $\tilde{\Psi}_i = \Psi_i - \hat{\Psi}_i$, $\hat{\Psi}_i$ denotes the estimation of Ψ_i, $\Psi_i = \|Y_i\|^2$, $i = 1, \ldots, n$.

Design α_i and $\dot{\hat{\Psi}}_i$ as

$$\alpha_1 = -\frac{\bar{\mathscr{C}}_1 z_1}{\mathcal{K}} - \frac{\mathcal{K} z_1 \hat{\Psi}_1}{2a_1 \mathscr{C}_0^{2\epsilon}} \tag{22}$$

$$\alpha_i = -\bar{\mathscr{C}}_i z_i - \frac{z_i \hat{\Psi}_i}{2a_i \mathscr{C}_0^{2\epsilon}}, i = 2, \ldots, n \tag{23}$$

$$\dot{\hat{\Psi}}_1 = \frac{r_1 \mathcal{K}^2 z_1^2}{2a_1 \mathscr{C}_0^{4\epsilon}} - \bar{\mathscr{C}}_1 \hat{\Psi}_1 \tag{24}$$

$$\dot{\hat{\Psi}}_i = \frac{r_i z_i^2}{2a_i \mathscr{C}_0^{4\epsilon}} - \bar{\mathscr{C}}_i \hat{\Psi}_i, i = 2, \ldots, n \tag{25}$$

where $\bar{\mathscr{C}}_i = k_i + \dot{\mathscr{C}}(t)/\mathscr{C}(t)$, $k_i, a_i, r_i \in R^+$ stand for the design parameters.

Step 1 : The first LF candidate (LFc) $\mathscr{L}_1$ is chosen as

$$\mathscr{L}_1 = \mathscr{L}_0 + \frac{1}{2\mathscr{C}_0^{2\epsilon}} z_1^2 + \frac{1}{2r_1} \tilde{\Psi}_1^2. \tag{26}$$

From (19), one has

$$\dot{\xi} = \mathcal{K} \dot{x}_1 + \upsilon \tag{27}$$

with

$$\mathcal{K} = \frac{\chi_1^2 - \bar{\mathscr{B}}\underline{\mathscr{B}}}{\left(\chi_1 - \underline{\mathscr{B}}\right)^2 \left(\bar{\mathscr{B}} - \chi_1\right)^2}$$

$$\upsilon = \frac{x_1 \left[\left(2\chi_1 - \underline{\mathscr{B}} - \bar{\mathscr{B}}\right) \dot{\mathscr{S}} x_1 - \left(\chi_1 - \bar{\mathscr{B}}\right) \dot{\underline{\mathscr{B}}} - \left(\chi_1 - \underline{\mathscr{B}}\right) \dot{\bar{\mathscr{B}}}\right]}{\left(\chi_1 - \underline{\mathscr{B}}\right)^2 \left(\bar{\mathscr{B}} - \chi_1\right)^2}.$$

Substituting (1) and (8) to (27), one can obtain

$$\dot{\xi} = \mathcal{K}\left(f_1(x_1) + \tilde{x}_2 + z_2 + \alpha_1 + \frac{\upsilon}{\mathcal{K}}\right). \tag{28}$$

From (17), (26) and (28), we have

$$\dot{\mathscr{L}}_1 \leq -\left[(n+1)\mathscr{C}_0 - 1 - \Theta\right] \|\eta\|^2 + \Delta_0 + \frac{\mathcal{K} z_1 \left(\bar{f}_1 + \tilde{x}_2 + \alpha_1\right)}{\mathscr{C}_0^{2\epsilon}} - \frac{\tilde{\Psi}_1 \dot{\hat{\Psi}}_1}{r_1} \tag{29}$$

where $\bar{f}_1 = f_1(x_1) + (\upsilon - \dot{\alpha}_0)/\mathcal{K} + z_2 - (\epsilon \dot{\mathscr{C}}_0 z_1)/(\mathcal{K}\mathscr{C}_0)$.

Based on Young's inequality, one has

$$\frac{\mathcal{K} z_1 \tilde{x}_2}{\mathscr{C}_0^{2\epsilon}} \leq \frac{\mathcal{K}^2 z_1^2}{4\mathscr{C}_0^{2\epsilon-1}} + \mathscr{C}_0 \|\eta\|^2. \tag{30}$$

Then, we have

$$\dot{\mathscr{L}}_1 \leq -\left(n\mathscr{C}_0 - 1 - \Theta\right) \|\eta\|^2 + \frac{\mathcal{K} z_1 \left(\mathcal{F}_1(\mathcal{Z}_1) + \alpha_1\right)}{\mathscr{C}_0^{2\epsilon}} - \frac{\mathcal{K}^2 z_1^2}{\mathscr{C}_0^{4\epsilon}} - \frac{\tilde{\Psi}_1 \dot{\hat{\Psi}}_1}{r_1} + \Delta_0 \tag{31}$$

where $\mathcal{Z}_1 = \left[x_1, \hat{x}_2, y_d\right]^{\mathrm{T}}$, $\mathcal{F}_1\left(\mathcal{Z}_1\right) = \bar{f}_1 + (\mathscr{C}_0\mathcal{K}z_1)/4 + (\mathcal{K}z_1)/\mathscr{C}_0^{2\epsilon}$.

On the basis of Lemma 2, a FLS is applied to approximate $\mathcal{F}_i\left(\mathcal{Z}_i\right)$, i.e., $\mathcal{F}_i\left(\mathcal{Z}_i\right) = Y_i^{\mathrm{T}}\Omega_i\left(\mathcal{Z}_i\right) + \phi_i\left(\mathcal{Z}_i\right)$, where $|\phi_i\left(\mathcal{Z}_i\right)| \le \phi_i$, and $\phi_i \in R^+$.

According to the mean inequality, one has

$$\frac{\mathcal{K}z_1\mathcal{F}_1\left(\mathcal{Z}_1\right)}{\mathscr{C}_0^{2\epsilon}} \le \frac{\mathcal{K}^2 z_1^2\Psi_1}{2a_1\mathscr{C}_0^{4\epsilon}} + \frac{\mathcal{K}^2 z_1^2}{\mathscr{C}_0^{4\epsilon}} + \bar{\Delta}_1 \tag{32}$$

where $\bar{\Delta}_1 = a_1/2 + \phi_1^2/4$, $a_1 \in R^+$.

Substituting (22), (24) and (32) to (31), we have

$$\dot{\mathscr{L}}_1 \le -\left(n\mathscr{C}_0 - 1 - \Theta\right)\|\eta\|^2 - \frac{\bar{\mathscr{C}}_1 z_1^2}{\mathscr{C}_0^{2\epsilon}} + \frac{\bar{\mathscr{C}}_1}{r_1}\tilde{\Psi}_1\hat{\Psi}_1 + \Delta_1 \tag{33}$$

where $\Delta_1 = \Delta_0 + \bar{\Delta}_1$.

Step i ($i = 2, \ldots, n-1$) : The ith LFc $\mathscr{L}_i$ is chosen as

$$\mathscr{L}_i = \frac{1}{2\mathscr{C}_0^{2(i-1+\epsilon)}}z_i^2 + \frac{1}{2r_i}\tilde{\Psi}_i^2 + \mathscr{L}_{i-1}. \tag{34}$$

Then, one can obtain

$$\dot{\mathscr{L}}_i \le \frac{z_i\left(\bar{f}_i + l_i\mathscr{C}_0^i\tilde{x}_1 + \alpha_i\right)}{\mathscr{C}_0^{2(i-1+\epsilon)}} - \frac{\tilde{\Psi}_i\dot{\hat{\Psi}}_i}{r_i} + \dot{\mathscr{L}}_{i-1} \tag{35}$$

where $\bar{f}_i = z_{i+1} - \dot{\alpha}_{i-1} - [(i-1+\epsilon)\dot{\mathscr{C}}_0 z_i]/\mathscr{C}_0$.

Similar to (30), we can get

$$\frac{z_i l_i\mathscr{C}_0^i\tilde{x}_1}{\mathscr{C}_0^{2(i-1+\epsilon)}} \le \frac{l_i^2 z_i^2}{4\mathscr{C}_0^{2i-4+2\epsilon}} + \|\eta\|^2. \tag{36}$$

Substituting (36) to (35), one can obtain

$$\dot{\mathscr{L}}_i \le \dot{\mathscr{L}}_{i-1} + \|\eta\|^2 + \frac{z_i\left(\mathcal{F}_i\left(\mathcal{Z}_i\right) + \alpha_i\right)}{\mathscr{C}_0^{2(i-1+\epsilon)}} - \frac{z_i^2}{\mathscr{C}_0^{4(i-1+\epsilon)}} - \frac{\tilde{\Psi}_i\dot{\hat{\Psi}}_i}{r_i} \tag{37}$$

where $\mathcal{F}_i\left(\mathcal{Z}_i\right) = \bar{f}_i + z_i/\mathscr{C}_0^{2(i-1+\epsilon)} + (\mathscr{C}_0^2 l_i^2 z_i)/4$, $\mathcal{Z}_i = \left[x_1, \hat{x}_2, \ldots, \hat{x}_{i+1}, y_d\right]^{\mathrm{T}}$.

Similar to (32), one can obtain

$$\frac{z_i\mathcal{F}_i\left(\mathcal{Z}_i\right)}{\mathscr{C}_0^{2(i-1+\epsilon)}} \le \frac{z_i^2\Psi_i}{2a_i\mathscr{C}_0^{4(i-1+\epsilon)}} + \frac{z_i^2}{\mathscr{C}_0^{4(i-1+\epsilon)}} + \bar{\Delta}_i \tag{38}$$

where $\bar{\Delta}_i = a_i/2 + \phi_i^2/4$, $a_i \in R^+$.

Substituting (23), (25) and (38) into (37), one can get

$$\dot{\mathscr{L}}_i \le -\left[(n-i+1)\mathscr{C}_0 - 1 - \Theta\right]\|\eta\|^2 - \sum_{j=1}^{i}\frac{\bar{\mathscr{C}}_j z_j^2}{\mathscr{C}_0^{2(j-1+\epsilon)}} + \sum_{j=1}^{i}\frac{\bar{\mathscr{C}}_j}{r_j}\tilde{\Psi}_j\hat{\Psi}_j + \Delta_i \tag{39}$$

where $\Delta_i = \sum_{j=1}^{i}\bar{\Delta}_j + \Delta_0$.

Step n : Introduce the following relative threshold-based event triggering mechanism

$$w(t) = -(1+m)\left[\alpha_n\tanh\left(\frac{z_n\alpha_n}{\rho}\right) + \tau\tanh\left(\frac{z_n\tau}{\rho}\right)\right] \tag{40}$$

$$u(t) = w(t_k), t_k \le t < t_{k+1} \tag{41}$$

$$t_{k+1} = \inf\left\{t > t_k \mid |\kappa(t)| \ge m|u(t)| + m_1\right\} \tag{42}$$

where $\kappa(t) = w(t) - u(t)$, t_k represents the instances of event triggers, $k \in \mathbb{Z}^+$, and $\rho, m_1 \in R^+$, $m \in (0,1)$, $\tau > m_1/(1-m)$.

For $\forall t \in [t_k, t_{k+1})$, one can know from (42) that

$$w(t) = [1 + \kappa_1(t)m]u(t) + \kappa_2(t)m_1 \tag{43}$$

with $-1 \le \kappa_1(t), \kappa_2(t) \le 1$.

Then

$$u(t) = \frac{w(t)}{1 + \kappa_1(t)m} - \frac{\kappa_2(t)m_1}{1 + \kappa_1(t)m}. \tag{44}$$

The nth LFc $\mathscr{L}_n$ is chosen as

$$\mathscr{L}_n = \frac{1}{2\mathscr{C}_0^{2(n-1+\epsilon)}} z_n^2 + \frac{1}{2r_n}\tilde{\Psi}_n^2 + \mathscr{L}_{n-1}. \tag{45}$$

We can get further

$$\begin{aligned}\dot{\mathscr{L}}_n \leq & \frac{z_n\left(\bar{f}_n + l_n\mathscr{C}_0^n\tilde{x}_1 + u(t)\right)}{\mathscr{C}_0^{2(n-1+\epsilon)}} - \frac{\tilde{\Psi}_n\dot{\hat{\Psi}}_n}{r_n} + \dot{\mathscr{L}}_{n-1} \\ \leq & \frac{z_n\left(\bar{f}_n + l_n\mathscr{C}_0^n\tilde{x}_1\right)}{\mathscr{C}_0^{2(n-1+\epsilon)}} + \frac{z_n\left(w(t) - \kappa_2(t)m_1\right)}{\mathscr{C}_0^{2(n-1+\epsilon)}\left(1+\kappa_1(t)m\right)} - \frac{\tilde{\Psi}_n\dot{\hat{\Psi}}_n}{r_n} + \dot{\mathscr{L}}_{n-1}\end{aligned} \tag{46}$$

where $\bar{f}_n = -\dot{\alpha}_{n-1} - [(n-1+\epsilon)\dot{\mathscr{C}}_0 z_n]/\mathscr{C}_0$.

Similar to (30) and (36), one has

$$\frac{z_n l_n\mathscr{C}_0^n\tilde{x}_1}{\mathscr{C}_0^{2(n-1+\epsilon)}} \leq \frac{l_n^2 z_n^2}{4\mathscr{C}_0^{2n-4+2\epsilon}} + \|\eta\|^2. \tag{47}$$

Substituting (47) to (46), we have

$$\dot{\mathscr{L}}_n \leq \frac{z_n\mathcal{F}_n\left(\mathcal{Z}_n\right)}{\mathscr{C}_0^{2(n-1+\epsilon)}} + \frac{z_n\left(w(t) - \kappa_2(t)m_1\right)}{\mathscr{C}_0^{2(n-1+\epsilon)}\left(1+\kappa_1(t)m\right)} - \frac{z_n^2}{\mathscr{C}_0^{4(n-1+\epsilon)}} - \frac{\tilde{\Psi}_n\dot{\hat{\Psi}}_n}{r_n} + \dot{\mathscr{L}}_{n-1} + \|\eta\|^2 \tag{48}$$

where $\mathcal{F}_n\left(\mathcal{Z}_n\right) = \bar{f}_n + z_n/\mathscr{C}_0^{2(n-1+\epsilon)} + (\mathscr{C}_0^2 l_n^2 z_n)/4$, $\mathcal{Z}_n = \left[x_1, \hat{x}_2, \ldots, \hat{x}_n, y_d\right]^{\mathrm{T}}$.

Similar to (32) and (38), one can obtain

$$\frac{z_n\mathcal{F}_n\left(\mathcal{Z}_n\right)}{\mathscr{C}_0^{2(n-1+\epsilon)}} \leq \frac{z_n^2\Psi_n}{2a_n\mathscr{C}_0^{4(n-1+\epsilon)}} + \frac{z_n^2}{\mathscr{C}_0^{4(n-1+\epsilon)}} + \bar{\Delta}_n \tag{49}$$

where $\bar{\Delta}_n = a_n/2 + \phi_n^2/4$, $a_n \in R^+$.

Since $\rho > 0$ and $-\tau\tanh(\tau/\rho) \leq 0$, one can obtain that $z_n\omega(t) \leq 0$. Consequently, we derive

$$\frac{z_n w(t)}{\mathscr{C}_0^{2(n-1+\epsilon)}\left(1+\kappa_1(t)m\right)} \leq \frac{z_n w(t)}{\mathscr{C}_0^{2(n-1+\epsilon)}(1+m)} \tag{50}$$

$$\frac{-z_n\kappa_2(t)m_1}{\mathscr{C}_0^{2(n-1+\epsilon)}\left(1+\kappa_1(t)m\right)} \leq \left|\frac{z_n m_1}{\mathscr{C}_0^{2(n-1+\epsilon)}(1-m)}\right|. \tag{51}$$

According to (48)–(51), one can obtain

$$\begin{aligned}\dot{\mathscr{L}}_n \leq & \frac{z_n^2\Psi_n}{2a_n\mathscr{C}_0^{4(n-1+\epsilon)}} + \left|\frac{z_n m_1}{\mathscr{C}_0^{2(n-1+\epsilon)}(1-m)}\right| - \frac{\tilde{\Psi}_n\dot{\hat{\Psi}}_n}{r_n} + \dot{\mathscr{L}}_{n-1} + \|\eta\|^2 + \bar{\Delta}_n \\ & - \frac{z_n}{\mathscr{C}_0^{2(n-1+\epsilon)}} \times \left[\alpha_n\tanh\left(\frac{z_n\alpha_n}{\rho}\right) + \tau\tanh\left(\frac{z_n\tau}{\rho}\right)\right]\end{aligned} \tag{52}$$

Utilizing the properties of the hyperbolic tangent function and $\tau > m_1/(1-m)$, it is established that

$$\dot{\mathscr{L}}_n \leq \frac{z_n^2\Psi_n}{2a_n\mathscr{C}_0^{4(n-1+\epsilon)}} - \frac{\tilde{\Psi}_n\dot{\hat{\Psi}}_n}{r_n} + \dot{\mathscr{L}}_{n-1} + \|\eta\|^2 + \frac{z_n\alpha_n}{\mathscr{C}_0^{2(n-1+\epsilon)}} + 0.557\rho\tau + \bar{\Delta}_n \tag{53}$$

Substituting (23) and (25) into (53), one can obtain

$$\dot{\mathscr{L}}_n \leq -\left(\mathscr{C}_0 - 1 - \Theta\right)\|\eta\|^2 + \Delta_n - \sum_{j=1}^{n}\frac{\bar{\mathscr{C}}_j z_j^2}{\mathscr{C}_0^{2(j-1+\epsilon)}} + \sum_{j=1}^{n}\frac{\bar{\mathscr{C}}_j}{r_j}\tilde{\Psi}_j\dot{\hat{\Psi}}_j \tag{54}$$

where $\Delta_n = \Delta_0 + 0.557\rho\tau + \sum_{j=1}^{n}\left(\phi_j/4 + a_j/2\right)$.

Since $\tilde{\Psi}_j\dot{\hat{\Psi}}_j \leq -\tilde{\Psi}_j^2/2 + \Psi_j^2/2$, one can obtain

$$\dot{\mathscr{L}}_n \leq -\left(\mathscr{C}_0 - 1 - \Theta\right)\|\eta\|^2 + \delta - \sum_{j=1}^{n}\frac{\bar{\mathscr{C}}_j z_j^2}{\mathscr{C}_0^{2(j-1+\epsilon)}} - \sum_{j=1}^{n}\frac{\bar{\mathscr{C}}_j\tilde{\Psi}_j^2}{2r_j} \tag{55}$$

where $\delta = \Delta_n + \sum_{j=1}^{n}\left(\bar{\mathscr{C}}_j\Psi_j^2\right)/\left(2r_j\right)$.

Let $k = \min_{1\leq i\leq n}\left\{k_i, \bar{k}_0 - (1+\Theta)/\lambda_{\min B}\right\}$ with $\bar{k}_0 > (1+\Theta)/\lambda_{\min B}$. One can know from the expression of $\bar{\mathscr{C}}_i$ that

$$\dot{\mathscr{L}}_n \leq -k\mathscr{L}_n - \frac{\dot{\mathscr{C}}(t)}{\mathscr{C}(t)}\mathscr{L}_n + \delta. \tag{56}$$

Fig. 1 gives the algorithm flow chart of this article.

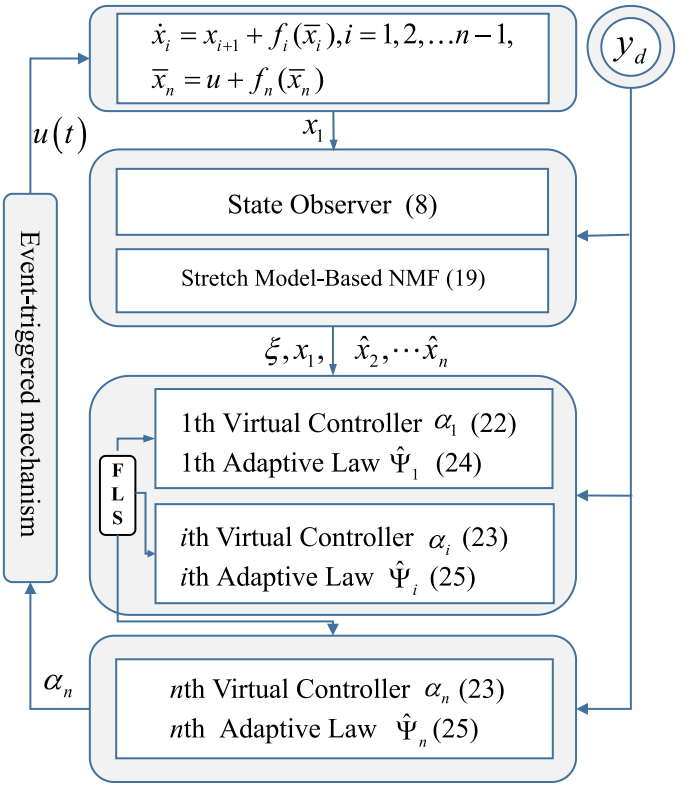

Fig. 1. Algorithm flow chart of this article.

3.3. Stability analysis

Theorem. For irregular OCNSs (1) with $x_1(0) \in \mathscr{B}_{x_1}$ and Assumptions 1–2, the designed event-based PTOFC algorithm ensures

(1) All the signals of system (1) are bounded.
(2) The system output is capable of tracking the reference signal y_d with a small tracking accuracy within the specified time t_f, and the irregular output constraints are being maintained.
(3) The Zeno behavior is avoided.

Proof. (1) From (56), we have

$$\mathscr{L}_n \leq \frac{\mathscr{L}_n(0)\, e^{-t}}{(1+\varepsilon)\mathscr{C}(t)} + \frac{\delta}{k\varepsilon\mathscr{C}(t)}. \tag{57}$$

It is not difficult to see from (57) and $\mathscr{L}_n$ that the boundedness of η_i, z_i and $\tilde{\Psi}_i$ can be ensured, and that the boundedness of α_i, u, $\hat{\Psi}_i$ and $\tilde{x}_i$ can be further ensured by (10), (22)–(25), then ξ and $\hat{x}_i$ are bounded. Since $x_i = \tilde{x}_i + \hat{x}_i$, one know that x_i is bounded. Thus, the boundedness of all closed-loop signals can be ensured.

(2) It can be further obtained from (57) and the expression of $\mathscr{C}(t)$ that

$$\mathscr{L}_n \leq \varepsilon\mathscr{L}_n(0) + \frac{\delta}{k}, \forall t \geq t_f. \tag{58}$$

According to the expression of $\mathscr{L}_n$ and (58), one has

$$|z_1| \leq \sqrt{2\left(\varepsilon\mathscr{L}_n(0) + \frac{\delta}{k}\right)}, \forall t \geq t_f. \tag{59}$$

Since

$$z_1 = \frac{e_1\left(\chi_1 y_d \mathscr{S} - \underline{\mathscr{B}}\bar{\mathscr{B}}\right)}{\left(\chi_1 - \underline{\mathscr{B}}\right)\left(\bar{\mathscr{B}} - \chi_1\right)\left(y_d\mathscr{S} - \underline{\mathscr{B}}\right)\left(\bar{\mathscr{B}} - y_d\mathscr{S}\right)}$$

with $e_1 = x_1 - y_d$, which means that e_1 also converge to a neighborhood centered on 0 within the specified time t_f. In other words, the system output is capable of tracking the reference signal y_d with a small tracking accuracy within the specified time t_f.

In addition, $x_1(0) \in \mathscr{B}_{x_1}$ means $\underline{\mathscr{B}}(0) < \chi_1(0) < \bar{\mathscr{B}}(0)$. Combining the boundedness of ξ and (19), one has

$$\underline{\mathscr{B}}(t) < \chi_1(t) < \bar{\mathscr{B}}(t). \tag{60}$$

It can be obtained from (60) and the properties of $\mathscr{S}$ that for $\forall t \in [t_{s,j}, t_{e,j}]$, $\underline{\mathscr{B}} < x_1 < \bar{\mathscr{B}}$, and when t belongs to a large measure subset of $(0, t_{s,1}) \cup \ldots (t_{e,j}, t_{s,j+1}) \cdots \cup (t_{e,k}, +\infty)$, the constraint boundaries $\underline{\mathscr{B}}(t)/\mathscr{S}(t)$ and $\bar{\mathscr{B}}(t)/\mathscr{S}(t)$ tend to infinity (i.e., $-\infty < x_1 < +\infty$), meaning that the irregular output constraints are being maintained.

(3) On the basis of the boundedness of the closed-loop signal, we can get $|\dot{w}(t)| \le \bar{w}$ with $\bar{w} \in R^+$. According to (41) and (42), one know that $\kappa(t_k) = 0$ and $\lim_{t \to t_{k+1}^{-1}} |\kappa(t)| = mu(t_k) + m_1$. Then one has $t_{k+1} - t_k \ge (mu(t_k) + m_1)/\bar{w} \ge m_1/\bar{w}$, meaning that $\inf\{t_{k+1} - t_k\} \ge m_1/\bar{w}$. Thus, the Zeno behavior is avoided. ■

Remark 6. The "uniformity" of the presented algorithm is its suitability for OCNSs with infinite-time/deferred/alternate output constraints, and unconstrained systems, without necessitating modifications to the control structure.

- If select $0 = t_{s,1} < t_{e,1} = +\infty$, then $\mathscr{S} \equiv 1$ holds $\forall t \in [0, +\infty)$, which indicates that the presented algorithm can effectively handle infinite-time output constraints [23–27];
- If select $0 < t_0 = t_{s,1} < t_{e,1} = +\infty$, meaning that for $t \in [0, t_0)$, there are no constraints, and the system encounters constraints when $t \in [t_0, +\infty)$. This effectively equivalent to the deferred output constraints [28–30], indicating that the presented algorithm can effectively handle deferred output constraints.
- If replace x_1 in (19) with e_1; replace the constraint function with "funnel function (or performance function)", and select $0 = t_{s,1} < t_{e,1} = +\infty$, the proposed method turns into the funnel (or prescribed performance) control problem [52–54]. Furthermore, if select $0 < t_0 = t_{s,1} < t_{e,1} = +\infty$, then the proposed method turns into the deferred funnel (or prescribed performance) control problem, which implies that the presented algorithm also can degenerate into prescribed-time funnel control of deferred OCNSs. If select $m = 1$, then the presented algorithm is reduced to the result in [19],i.e., "unconstrained→ constrained→ unconstrained".
- If select $t_{s,1} = +\infty$, one can know from Remark 4 that $\underline{\mathscr{B}}/\mathscr{S} \to -\infty, \bar{\mathscr{B}}/\mathscr{S} \to +\infty$, indicating that the presented algorithm also suit for unconstrained nonlinear systems.

Remark 7. Note that the proposed algorithm contains some control parameters. According to the stability analysis, the selection of these parameters in practice follows the following rules: increasing k_i and r_i or decreasing a_i can reduce the tracking error, i.e., improve the tracking performance. Users can adjust parameter t_f to set the system stability time as required. Of course, in practice, the parameters need to be combined with the system structure and actual performance requirements for general debugging.

4. Simulation

Example 1 (*Theoretical system*).: Give a system as follows

$$\begin{cases} \dot{x}_1 = x_2 + \sin x_1^2 \cos x_1 \\ \dot{x}_2 = u + x_1\left(1 + x_2^2\right)\sin x_2 - 1.2x_1x_2 \\ y = x_1. \end{cases} \tag{61}$$

The design parameters are selected as $k_1 = 80, k_2 = 3, a_i = 10, r_i = 50, l_i = 1$ with $i = 1, 2$, $\epsilon = \delta_j^i = 0.0001$, $t_f = 5$, $\underline{\mathscr{B}} = 0.1\sin t - 0.7$, $\bar{\mathscr{B}} = 0.1\sin t + 0.7$, $t_{s,1} = 4, t_{e,1} = 9, t_{s,2} = 16, t_{e,2} = 21$. Let $y_d = 0.5\sin(0.5t) + \sin t$, and $\hat{\Psi}_1(0) = 3$, $\hat{\Psi}_2(0) = 2$, $\bar{x}_2(0) = [0.5, 0.2]^{\mathrm{T}}$. Choose the fuzzy membership functions as: $\Omega_i = e^{-(\mathcal{Z}_i - 5 + j)^2/2}, i = 1, 2, j = 1, \ldots, 9$. It can be known from subgraphs (a)–(d) of Fig. 2 that y tracks y_d within t_f, while also maintaining compliance with the irregular output constraints. The curves of u and $w(t)$ are given in subgraph (e) of Fig. 2, and the curve of the inter-execution interval is given in subgraph (f) of Fig. 2.

We compare the proposed method with that in [27] (infinite-time output constraints) to highlight the merits of the presented method. Let $y_d = 0.5\sin(2t) + \sin(t)$, and we select three different initial outputs: case 1: $x_1 = 2.5$; case 2: $x_1 = 0.2$; case 3: $x_1 = -2$. One can know from subgraph (a) of Fig. 3 that the system can run normally if and only if the initial output is within the constraint boundaries, which implying that the method proposed in [27] is obviously very conservative, i.e., when the initial output changes, it needs to be verified again whether it belongs to the constraint boundaries, if not, the method is no longer applicable. However, according to (b) of Fig. 3, by setting $t_{s,1}$ to a small positive constant, the proposed method "stretches" the initial constraint boundaries to the infinite boundaries, resulting in the proposed method being suitable for constraint problems with any initial output.

In addition, we also present a comparison with the approach presented in [52]. Replace x_1 in (19) with e_1, $\alpha_0 = 0$. It is evident that if $\mathscr{S} \equiv 1$, the approach employed to manage the irregular output constraints in this article reduces to the method presented in [52] (funnel or prescribed performance control). Note that for the method in [52], the initial error needs to be satisfied $e_1(0) \in (\underline{\mathscr{B}}(0), \bar{\mathscr{B}}(0))$. However, in contrast to the approach presented in [52], a significant advantage of our method is that it is applicable to any bounded initial error. To verify this, we choose three different initial errors: Case 1: $e_1(0) = 2.5$; Case 2: $e_1 = 1$; Case 3: $e_1 = -2.5$. Let $t_{s,1} = 1, t_{e,1} = +\infty$. One can see from subgraphs (a) and (b) of Fig. 4 that the method presented in [52] applies only to case 2, the proposed algorithm, however, remains efficacious for all three cases. Additionally, the approach presented in [52] fails to account for the settling time, whereas the proposed method guarantees stability within a prescribed time.

To substantiate the superiority of the presented PTOFC approach, we conduct a comparative analysis with the approach presented in [49]. Let $y_d = 0.5\sin t$, $\bar{x}_2 = [1, 1.2]^{\mathrm{T}}$, $t_{s,1} = +\infty$ (i.e.,unconstrained situation). It can be inferred from Fig. 5 that the presented

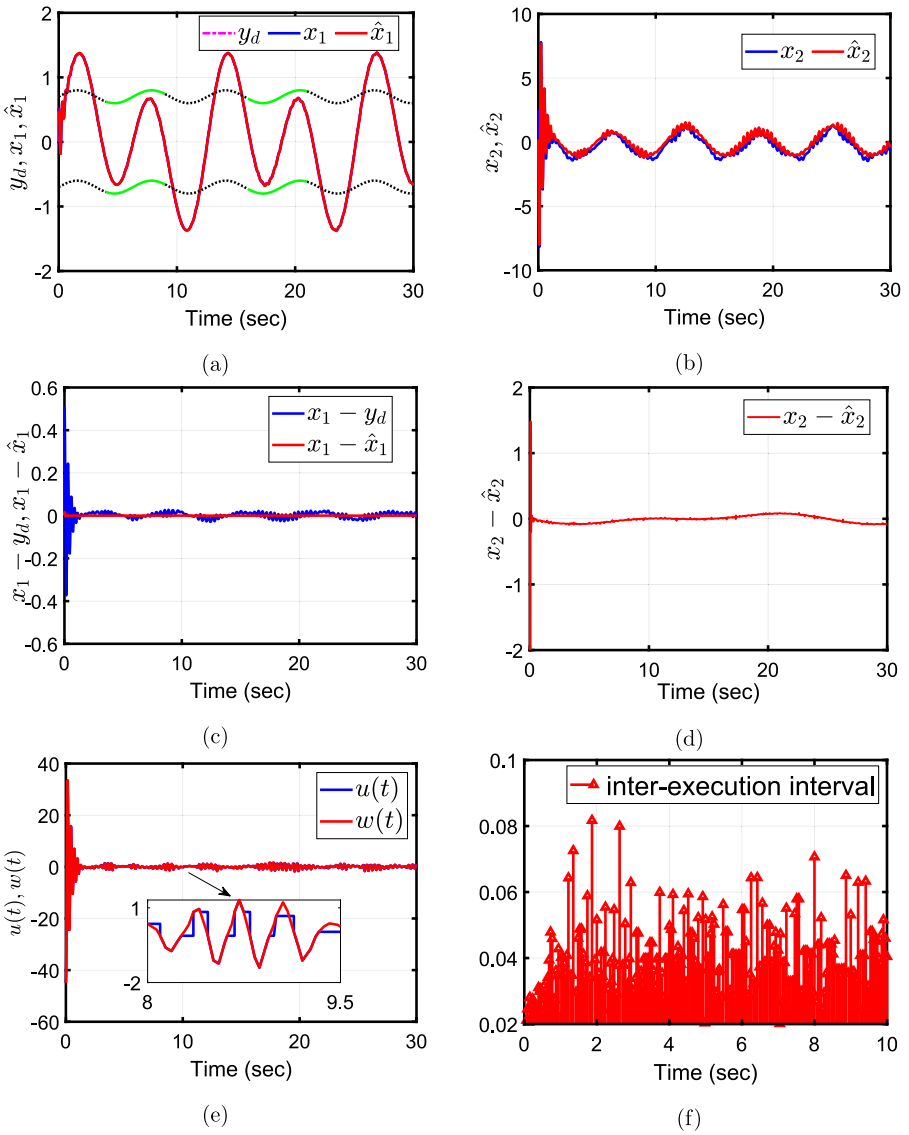

Fig. 2. (a) Curves of $y_d, x_1, \hat{x}_1$ (b) Curves of $x_2, \hat{x}_2$ (c) Curves of $x_1 - y_d, x_1 - \hat{x}_1$ (d) Curve of $x_2 - \hat{x}_2$ (e) Curves of $u(t)$ and $w(t)$ (f) Curve of the inter-execution interval.

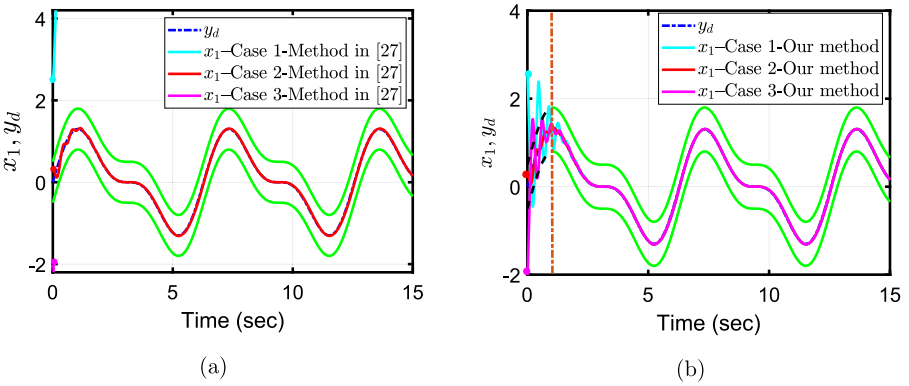

Fig. 3. (a) Tracking curves under the method in [27] with different initial outputs (b) Tracking curves under the proposed method with different initial outputs.

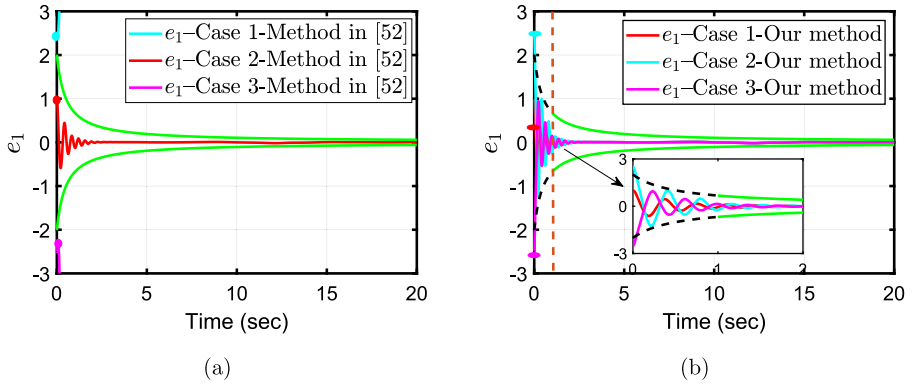

Fig. 4. (a) Tracking error curves under the method in [52] with different initial errors (b) Tracking error curves under the proposed method with different initial errors.

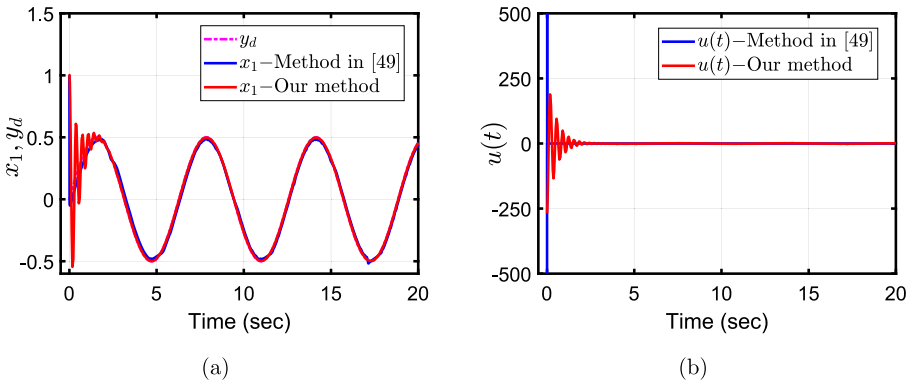

Fig. 5. (a) Tracking curves of the proposed method and that in [49] under the same initial conditions (b) Control inputs of the proposed method and that in [49] under the same initial conditions.

PTOFC approach is suit for nonlinear systems without output constraints. Moreover, the proposed PTOFC approach can attain comparable control performance as demonstrated in [49], while requiring significantly smaller initial control input than that of [49].

Example 2 (*Practical system*).: Consider a single-link robot arm system [16] as follows

$$\begin{cases} \dot{x}_1 = x_2 \\ \dot{x}_2 = \frac{-mgl\sin x_1}{2M} - \frac{Bx_2}{M} + \frac{u}{M} \\ y = x_1 \end{cases} \tag{62}$$

where $m = 0.02$ kg, $g = 9.8$ m/s^2, $l = 1$ m, $M = 1$ kg, $B = 1$.

Let $y_d = 0.5\cos(0.5t) - 0.4\sin(0.25t) - 0.25$, $k_1 = 80, k_2 = 3, a_i = 0.1, r_i = 50, l_i = 1$ with $i = 1, 2$, $\epsilon = \delta_j^i = 0.0001$, $t_f = 4$, $\underline{\mathscr{B}} = -0.4 + 0.01\sin t$, $\bar{\mathscr{B}} = 0.4 + 0.01\sin t$, $t_{s,1} = 10.5, t_{e,1} = 27, t_{s,2} = 35.5, t_{e,2} = 52, t_{s,3} = +\infty$, $\hat{\Psi}_1(0) = 3$, $\hat{\Psi}_2(0) = 2$, $\bar{x}_2(0) = [0.51, 0.5]^{\mathrm{T}}$. Choose the fuzzy membership functions as: $\Omega_i = e^{-(\bar{Z}_i - 5 + j)^2/2}, i = 1, 2, j = 1, \ldots, 9$. It can be known from subgraphs (a)–(d) of Fig. 6 that y tracks the y_d within t_f, while also maintaining compliance with the irregular output constraints. The curves of u and $w(t)$ are given in subgraph (e) of Fig. 2, and the curve of the inter-execution interval is given in subgraph (f) of Fig. 2.

We compare the proposed method with that in [27] (infinite-time output constraints). Let $y_d = 0.5\sin(2t) + \cos(t)$, and we select three different initial outputs: case 1: $x_1 = 2.5$; case 2: $x_1 = 1.1$; case 3: $x_1 = 0$. According to subgraph (a) of Fig. 7, one can see that the system can run normally if and only if the initial output is within the constraint boundaries. However, it can be seen from (b) of Fig. 7 that by setting $t_{s,1}$ to a small positive constant, the proposed method being suitable for constraint problems with any initial output. In addition, we also present a comparison with the approach presented in [52] (funnel or prescribed performance control). Replace x_1 in (19) with e_1, $\alpha_0 = 0$. We also choose three different initial errors: Case 1: $e_1(0) = 2.5$; Case 2: $e_1 = -1$; Case 3: $e_1 = -2.5$. Let $t_{s,1} = 1, t_{e,1} = +\infty$. One can see from subgraphs (a) and (b) of Fig. 8 that the method presented in [52] applies only to case 2, the proposed algorithm, however, remains efficacious for all three cases. Furthermore, we conduct a comparative analysis with the approach presented in [49]. Let $y_d = \sin(0.5t) + 0.5\sin t$, $\bar{x}_2 = [1.5, 1.2]^{\mathrm{T}}$, $t_{s,1} = +\infty$ (i.e.,unconstrained situation). One can infer from Fig. 9 that the presented PTOFC approach is suit for nonlinear systems without output constraints, and it can

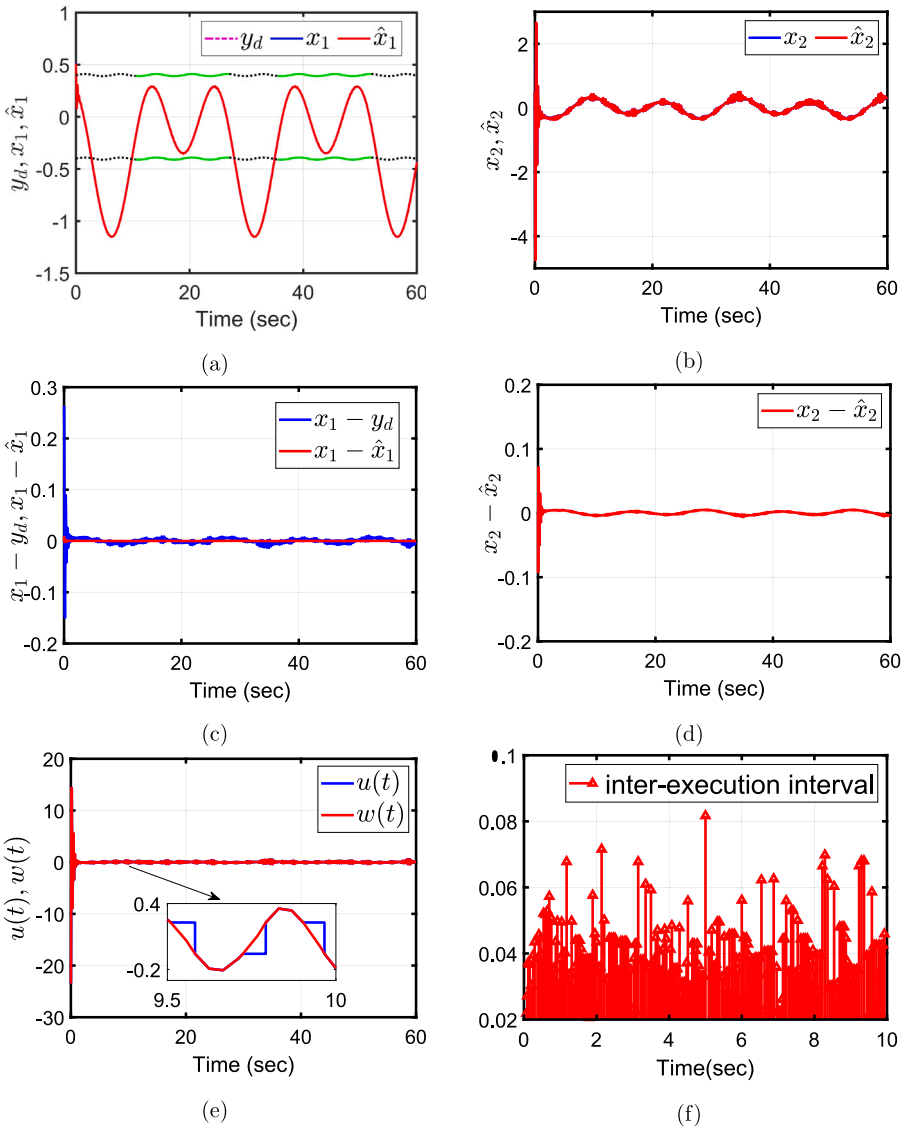

Fig. 6. (a) Curves of $y_d, x_1, \hat{x}_1$ (b) Curves of $x_2, \hat{x}_2$ (c) Curves of $x_1 - y_d, x_1 - \hat{x}_1$ (d) Curve of $x_2 - \hat{x}_2$ (e) Curves of $u(t)$ and $w(t)$ (f) Curve of the inter-execution interval.

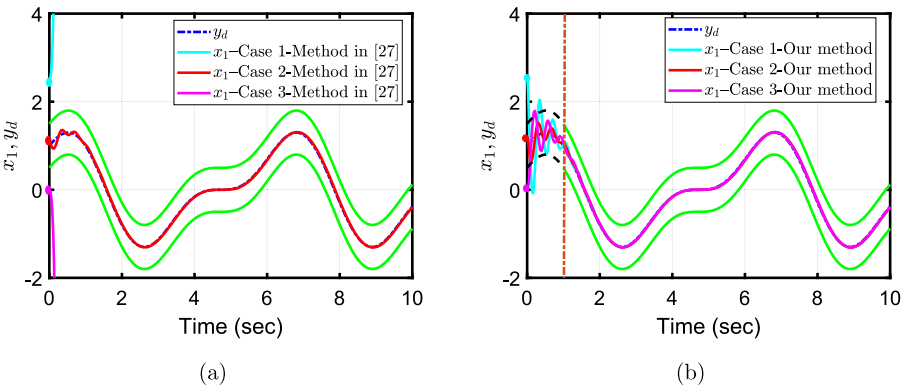

Fig. 7. (a) Tracking curves under the method in [27] with different initial outputs (b) Tracking curves under the proposed method with different initial outputs.

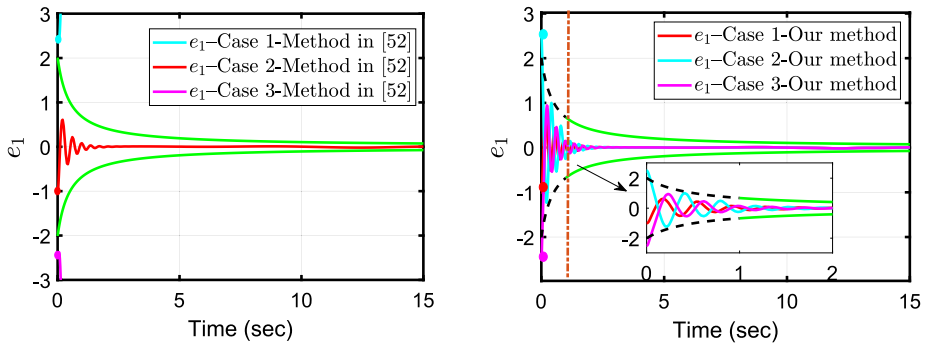

Fig. 8. (a) Tracking error curves under the method in [52] with different initial errors (b) Tracking error curves under the proposed method with different initial errors.

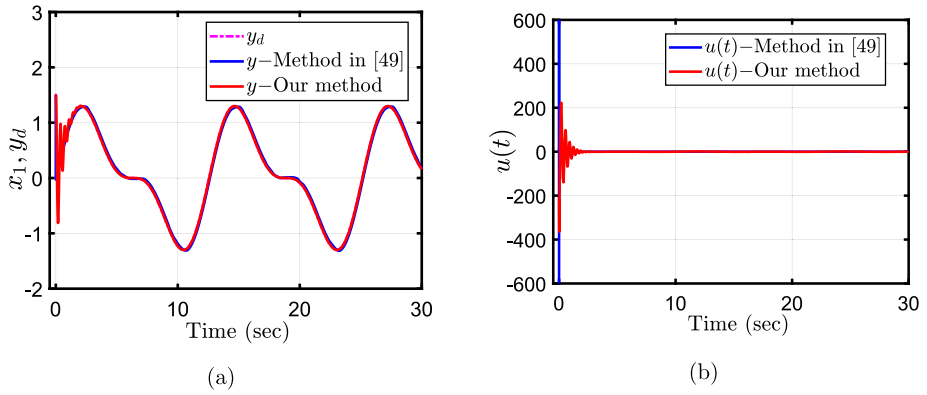

Fig. 9. (a) Tracking curves of the proposed method and that in [49] under the same initial conditions (b) Control inputs of the proposed method and that in [49] under the same initial conditions.

attain comparable control performance as demonstrated in [49], while requiring significantly smaller initial control input than that of [49].

5. Conclusion

In this article, a novel event-based uniform PTOFC algorithm for irregular OCNSs is presented, under which the settling time can be pre-set arbitrarily, regardless of the initial system states and control parameters. Meanwhile, the problems of singularity and large initial control input in conventional PTC algorithms are eliminated. The irregular output constraints are processed by devising a novel stretch model-based NMF, and the significant merit is its suitability for infinite-time/deferred/alternant OCNSs, and unconstrained systems, without necessitating modifications to the control structure. Our further focus will be on the event-based PTOFC and application of stochastic irregular OCNSs.

CRediT authorship contribution statement

Yangang Yao: Writing – original draft. **Yu Kang:** Writing – review & editing. **Yunbo Zhao:** Writing – review & editing. **Jieqing Tan:** Writing – review & editing. **Lichuan Gu:** Writing – review & editing. **Chao Wang:** Writing – review & editing.

Declaration of competing interest

The authors declare that they have no known competing financial interests or personal relationships that could have appeared to influence the work reported in this paper.

Acknowledgments

This work is supported in part by Anhui Provincial Department of Education Research Project under grant 2024AH040082; the Open Fund of State Key Laboratory of Tea Plant Biology and Utilization under grant SKLTOF20240112, the National Natural Science Foundation of China (62033012, 62103394, 62172135 and 32472007).

Data availability

No data was used for the research described in the article.

References

[1] Ngo K, Mahony R, Jiang Z. Integrator backstepping using barrier functions for systems with multiple state constraints. In: Proc. 44th IEEE conf decision control. 2005, p. 8306–12.
[2] Liu Y, Wang Y, Feng Y, Wu Y. Neural network-based adaptive boundary control of a flexible riser with input deadzone and output constraint. IEEE Trans Cybern 2022;52(12):13120–8.
[3] Zhao Z, Zhang J, Liu Z, Mu C, Hong K. Adaptive neural network control of an uncertain 2-DOF helicopter with unknown backlash-like hysteresis and output constraints. IEEE Trans Neural Netw Learn Syst 2023;34(12):10018–27.
[4] Lin X, Xue J, Zheng E, Park J. State-feedback stabilization for high-order output-constrained switched nonlinear systems. IEEE Trans Syst Man Cybern Syst 2022;52(12):7401–10.
[5] Ding S, Zhang B, Mei K, Park J. Adaptive fuzzy SOSM controller design with output constraints. IEEE Trans Fuzzy Syst 2022;30(7):2300–11.
[6] Tee K, Ren B, Ge S. Control of nonlinear systems with time-varying output constraints. Automatica 2011;47(11):2511–6.
[7] Zong G, Wang Y, Niu B, Su S, Shi K. Event-triggered adaptive NN tracking control for nonlinear systems with asymmetric time-varying output constraints and application to an AUVs. IEEE Trans Veh Technol 2025;74(1):413–24.
[8] Singh P, Giri D, Ghosh A. Dynamic surface neuro-backstepping based flight control with asymmetric output constraints. IEEE Trans Aerosp Electron Syst 2023;59(4):3859–70.
[9] Zhao K, Song Y. Removing the feasibility conditions imposed on tracking control designs for state-constrained strict-feedback systems. IEEE Trans Autom Control 2019;64(3):1265–72.
[10] Yao Y, Tan J, Wu J, Zhang X. A unified fuzzy control approach for stochastic high-order nonlinear systems with or without state wonstraints. IEEE Trans Fuzzy Syst 2022;30(10):4530–40.
[11] Yao Y, Kang Y, Zhao Y, Li P. Tan J. Unified fuzzy control of high-order nonlinear systems with multi-type state constraints. IEEE Trans Cybern 2024;54(4):2525–35.
[12] Yao Y, Tan J, Wu J, Zhang X. Decentralized fixed-time control for state-constrained stochastic systems via nonlinear state-dependent function approach. Internat J Robust Nonlinear Control 2022;32(8):4923–45.
[13] Yao Y, Tan J, Wu J, Zhang X. Event-triggered fixed-time adaptive fuzzy control for state-constrained stochastic nonlinear systems without feasibility conditions. Nonlinear Dynam 2021;105:403–16.
[14] Yao Y, Kang Y, Zhao Y, Tan J, Gu L, Shi G. Sliding flexible prescribed performance control for input saturated nonlinear systems. IEEE Trans Fuzzy Syst 2024. http://dx.doi.org/10.1109/TFUZZ.2024.3516132.
[15] Li Y, Ding S, Hua C, Chen J. Output-constrained consensus tracking for high-order nonlinear multiagent systems under switching networks. IEEE Trans Syst Man Cybern Syst 2023;53(12):7608–17.
[16] Zhao K, Chen L, Chen C. Event-based adaptive neural control of nonlinear systems with deferred constraint. IEEE Trans Syst Man Cybern Syst 2022;52(10):6273–82.
[17] Wu J, He F, Shen H, Ding S, Wu Z. Adaptive NN fixed-time fault-tolerant control for uncertain stochastic system with deferred output constraint via self-triggered mechanism. IEEE Trans Cybern 2023;53(9):5892–903.
[18] Liu S, Niu B, Zong G, Zhao X, Xu N. Adaptive neural dynamic-memory event-triggered control of high-order random nonlinear systems with deferred output constraints. IEEE Trans Autom Sci Eng 2024;21(3):2779–91.
[19] Kong L, He W, Liu Z, Yu X, Silvestre C. Adaptive tracking control with global performance for output-constrained MIMO nonlinear systems. IEEE Trans Autom Control 2023;68(6):3760–7.
[20] Yao Y, Kang Y, Zhao Y, Li P, Tan J. A novel prescribed-time control approach of state-constrained high-order nonlinear systems. IEEE Trans Syst Man Cybern Syst 2024. http://dx.doi.org/10.1109/TSMC.2024.3352905.
[21] Zhao K, Song Y. Decision function-based adaptive control of uncertain systems subject to irregular output constraints. IEEE Trans Autom Control 2024. http://dx.doi.org/10.1109/TAC.2024.3406580.
[22] Guo X, Zhang H, Yue X, Wang T. Optimized backstepping cooperative control for output-constrained stochastic nonlinear network systems via a multibridge-hole function. IEEE Trans Cybern 2024. http://dx.doi.org/10.1109/TCYB.2024.3384467.
[23] Yu X, He W, Li H, Sun J. Adaptive fuzzy full-state and output-feedback control for uncertain robots with output constraint. IEEE Trans Syst Man Cybern Syst 2021;51(11):6994–7007.
[24] Rincon K, Chairez I, Yu W. Finite-time output feedback robust controller based on tangent barrier lyapunov function for restricted state space for biped robot. IEEE Trans Syst Man Cybern Syst 2022;52(8):5042–55.
[25] Si C, Lam H, Liu J, Yu J. Event-triggered adaptive fuzzy finite-time output feedback control for stochastic nonlinear systems with input and output constraints. IEEE Trans Fuzzy Syst 2023;31(10):3555–66.
[26] Zuo R, Li Y, Lv M, Liu Z, Zhang F. Fuzzy adaptive output-feedback constrained trajectory tracking control for HFVs with fixed-time convergence. IEEE Trans Fuzzy Syst 2022;30(11):4828–40.
[27] Zhang C, Yu Y, Zhang X, Shen C, Su C, Zhou M. Predefined-time adaptive control of a piezoelectric-driven motion system with time-varying output constraint. IEEE Trans Circuits Syst II Exp Briefs 2023;70(7):2605–9.
[28] Wang A, Liu L, Qiu J, Feng G. Event-triggered adaptive fuzzy output-feedback control for nonstrict-feedback nonlinear systems with asymmetric output constraint. IEEE Trans Cybern 2022;52(1):712–22.
[29] Zhao K, Song Y, Chen C, Chen L. Adaptive asymptotic tracking with global performance for nonlinear systems with unknown control directions. IEEE Trans Autom Control 2022;67(3):1566–73.
[30] Meng R, Hua C, Li K, Ning P. A multifilters approach to adaptive event-triggered control of uncertain nonlinear systems with global output constraint. IEEE Trans Cybern 2024;52(2):1143–53.
[31] Polyakov A, Efimov D, Perruquetti W. Finite-time and fixed-time stabilization: implicit Lyapunov function approach. Automatica 2015;51:332–40.

[32] Wang Y, Zong G, Zhao X, Yi Y. Adaptive practical fixed-time synchronized tracking control of ASV with prescribed performance. Automatica 2024;111716.
[33] Wang Y, Zong G. Dynamic event-triggered adaptive fixed-time practical tracking control for nonlinear systems through funnel function. IEEE Trans Autom Sci Eng 2024;22:7008–17.
[34] Yao Y, Tan J, Wu J, Zhang X. Event-triggered fixed-time adaptive neural dynamic surface control for stochastic non-triangular structure nonlinear systems. Inf Sci 2021;569:527–43.
[35] Yao Y, Tan J, Wu J, Zhang X, He L. Prescribed tracking error fixed-time control of stochastic nonlinear systems. Chaos Solitons Fractals 2022;160:112288.
[36] Sánchez-Torres J, Sanchez E, Loukianov A. Predefined-time stability of dynamical systems with sliding modes.. In: 2015. American control conference. ACC, 2015, p. 5842–6.
[37] Song Y, Wang Y, Holloway J, Krstic M. Time-varying feedback for regulation of normal-form nonlinear systems in prescribed finite time. Automatica 2017;83:243–52.
[38] Hua C, Ning P, Li K. Adaptive prescribed-time control for a class of uncertain nonlinear systems. IEEE Trans Autom Control 2021;61(17):6159–66.
[39] Gao F, Wu Y, Zhang Z. Global fixed-time stabilization of switched nonlinear systems: a time-varying scaling transformation approach. IEEE Trans Circuits Syst II Exp Briefs 2019;66(11):1890–4.
[40] Pal A, Kamal S, Yu X, Nagar S, Xiong X. Free-will arbitrary time consensus for multiagent systems. IEEE Trans Cybern 2022;52(6):4636–46.
[41] Sheng Z, Ma Q, Xu S. Prescribed-time output feedback control for high-order nonlinear systems. IEEE Trans Circuits Syst II Exp Briefs 2023;70(7):2460–4.
[42] Li W, Krstic M. Stochastic nonlinear prescribed-time stabilization and inverse optimality. IEEE Trans Autom Control 2022;67(3):1179–93.
[43] Li W, Krstic M. Prescribed-time output-feedback control of stochastic nonlinear systems. IEEE Trans Autom Control 2023;68(3):1431–46.
[44] Ning B, Han Q, Zuo Z. Practical fixed-time consensus for integrator-type multi-agent systems: a time base generator approach. Automatica 2019;105:406–14.
[45] Zeng D, Liu Z, Chen C, Zhang Y, Wu Z. Adaptive fuzzy output-feedback predefined-time control of nonlinear switched systems with admissible edge-dependent average dwell time. IEEE Trans Fuzzy Syst 2022;30(12):5337–50.
[46] Wang Z, Lam H, Guo Y, Xiao B, Li Y, Su X, et al. Adaptive event-triggered control for nonlinear systems with asymmetric state constraints: a prescribed-time approach. IEEE Trans Autom Control 2023;68(6):3625–32.
[47] Wang Z, Lam H, Xiao B, Chen Z, Liang B, Zhang T. Event-triggered prescribed-time fuzzy control for space teleoperation systems subject to multiple constraints and uncertainties. IEEE Trans Fuzzy Syst 2021;29(9):2785–97.
[48] Xu H, Yu D, Sui S, Chen C. An event-triggered predefined time decentralized output feedback fuzzy adaptive control method for interconnected systems. IEEE Trans Fuzzy Syst 2023;31(2):631–44.
[49] Wang Q, Cao J, Liu H. Adaptive fuzzy control of nonlinear systems with predefined time and accuracy. IEEE Trans Fuzzy Syst 2022;30(12):5152–65.
[50] Zou A, Liu Y, Hou Z, Hu Z. Practical predefined-time output-feedback consensus tracking control for multiagent systems. IEEE Trans Cybern 2023;53(8):5311–22.
[51] Yao Y, Kang Y, Zhao Y, Li P, Tan J. Prescribed-time output feedback control for cyber–physical systems under output constraints and malicious attacks. IEEE Trans Cybern 2024. http://dx.doi.org/10.1109/TCYB.2024.3418384.
[52] Min X, Baldi S, Yu W, Cao J. Low-complexity control with funnel performance for uncertain nonlinear multi-agent systems. IEEE Trans Autom Control 2023. http://dx.doi.org/10.1109/TAC.2023.3302855.
[53] Yao Y, Kang Y, Zhao Y, Li P. Tan J. Flexible prescribed performance output feedback control for nonlinear systems with input saturation. IEEE Trans Fuzzy Syst 2024. http://dx.doi.org/10.1109/TFUZZ.2024.3418772.
[54] Yao Y, Liang X, Kang Y, Zhao Y, Tan J, Gu L. Dual flexible prescribed performance control of input saturated high-order nonlinear systems. IEEE Trans Cybern 2025;55(3):1147–58.